HHS Public Access

Author manuscript

J Invest Dermatol. Author manuscript; available in PMC 2023 November 01.

Published in final edited form as:

J Invest Dermatol. 2022 November ; 142(11): 2988–2997.e3. doi:10.1016/j.jid.2022.05.005.

Role of MrgprB2 in Rosacea-Like Inflammation in Mice: Modulation by β-Arrestin 2

Saptarshi Roy[1], **Ibrahim Alkanfari**[1,2], **Shaswati Chaki**[1], **Hydar Ali**[1]

[1]Department of Basic & Translational Sciences, School of Dental Medicine, University of Pennsylvania, Philadelphia, Pennsylvania, USA

[2]Faculty of Dentistry, King Abdulaziz University, Jeddah, Saudi Arabia

Abstract

Cathelicidin LL-37–mediated activation of mast cells (MCs) has been implicated in the pathogenesis of rosacea, but the receptor involved and the mechanism of its activation and regulation remain unknown. We found that skin biopsies from patients with rosacea display higher frequencies of MCs expressing MRGPRX2 (mouse counterpart MrgprB2) than normal skin. Intradermal injection of LL-37 in wild-type mice resulted in MC recruitment, expression of inflammatory mediators, and development of rosacea-like inflammation. These responses were substantially reduced in *MrgprB2*$^{-/-}$ mice and abolished in MC deficient W^{sh}/W^{sh} mice. β-arrestin 2 is an adaptor protein that regulates G protein—coupled receptor function by receptor desensitization and also by activation of downstream signaling. We found that LL-37–induced rosacea-like inflammation was significantly reduced in mice with MC-specific deletion of β-arrestin 2 compared with that in control mice. Interestingly, the absence of β-arrestin 2 resulted in enhanced cofilin phosphorylation and substantial inhibition of LL-37–induced chemotaxis of mouse peritoneal MCs. Furthermore, LL-37–induced extracellular signal–regulated kinase 1/2 phosphorylation, NF-κB activation, and proinflammatory cytokine/chemokine production were reduced in β-arrestin $2^{-/-}$ peritoneal MCs compared with those in wild-type cells. These findings suggest that MRGPRX2/B2 participates in rosacea and that β-arrestin 2 contributes to its pathogenesis by promoting cofilin dephosphorylation, extracellular signal–regulated kinase 1/2 and NF-κB phosphorylation, MC chemotaxis, and chemokine/cytokine generation.

INTRODUCTION

Mast cells (MCs) are tissue-resident immune cells that are found beneath the epithelia in close proximity to nerve endings and blood vessels and contribute to antimicrobial host

Correspondence: Hydar Ali, Department of Basic and Translational Sciences, School of Dental Medicine, University of Pennsylvania, 240 South 40th Street, Philadelphia, Pennsylvania 19104, USA. alih@upenn.edu.

AUTHOR CONTRIBUTIONS

Conceptualization: HA; Formal Analysis: SR, IA, SC; Investigation: SR, IA, SC; Methodology: SR, IA, SR; Supervision: HA; Writing – Original Draft Preparation: SR; Writing - Review and Editing: SR, HA.

CONFLICT OF INTEREST

The authors state no conflict of interest.

SUPPLEMENTARY MATERIAL

Supplementary material is linked to the online version of the paper at www.jidonline.org, and at https://doi.org/10.1016/j.jid.2022.05.005

defense (Roy et al., 2021). Rosacea is a chronic inflammatory skin condition that likely results from dysregulated host defense, excessive production of the antimicrobial peptide cathelicidin LL-37, and aberrant recruitment and activation of cutaneous MCs (Kanada et al., 2012; Muto et al., 2014; Yamasaki et al., 2007). Activated MCs generate proteases, which promote LL-37 production from the skin epidermis, thus providing a bidirectional interaction between these two cell types, contributing to the symptoms associated with rosacea (Muto et al., 2014). A previous study showed that LL-37 induces mediator release from a human MC line (LAD2 cells) through G protein–mediated signaling pathway (Niyonsaba et al., 2010). Subramanian et al. (2011) provided the first demonstration that LL-37 induces chemotaxis, degranulation, and chemokine generation in human MCs through the activation of a novel G protein–coupled receptor (GPCR) known as MRGPRX2. Although MC numbers are increased in the skin of patients with rosacea, the status of MRGPRX2 in rosacea has not been determined.

Much of our current understanding of MC's role in the pathogenesis of rosacea comes from studies with a murine model where rosacea-like inflammation is induced by intradermal injection of LL-37 (Yamasaki et al., 2007). In this model, the development of rosacea-like inflammation is associated with MC recruitment, increased expression of MC proteases, and the generation of chemokines and immune cell infiltration (Muto et al., 2014). Interestingly, these responses are absent in MC-deficient mice or in normal mice treated with agents that block LL-37–induced MC mediator release (Callahan et al., 2020; Choi et al., 2019; Dondalska et al., 2020; Muto et al., 2014). These findings suggest that activation of MCs by LL-37 plays a critical role in the pathogenesis of rosacea and rosacea-like inflammation in mice. *MrgprB2* was originally identified as the murine ortholog of human *MRGPRX2*, and both receptors are activated by the same group of ligands (McNeil et al., 2015). Although LL-37 activates human MCs through MRGPRX2 (Mascarenhas et al., 2017; Subramanian et al., 2011), the possibility that it activates MrgprB2 to cause rosacea-like inflammation in mice has not been determined.

In addition to G protein activation, most agonist-occupied GPCRs undergo phosphorylation, which results in the recruitment of adapter proteins β-arrestins (βarrs), resulting in receptor desensitization and internalization. In addition, βarrs act as transducers of various downstream signaling pathways independent of their effect on desensitization. It is noteworthy that LL-37 does not cause MRGPRX2 desensitization, but it promotes MC chemotaxis (Subramanian et al., 2011). For certain GPCRs, β-arrestin 2 (βarr2) orchestrates cytoskeletal rearrangement and cell migration by modulating the phosphorylation and dephosphorylation status of the actin depolymerization factor cofilin (McGovern and DeFea, 2014; Zoudilova et al., 2010). Cofilin phosphorylation at Ser-3 causes its inactivation, whereas dephosphorylation promotes its activation (Zoudilova et al., 2007, 2010). Furthermore, stimulation of β-adrenergic receptor causes βarr-dependent extracellular signal–regulated kinase 1/2 (ERK1/2) phosphorylation, independent of its G protein activation (Shenoy et al., 2006). In addition, βarr2 plays a critical role in a mouse model of allergic asthma, and this effect results from its ability to promote NF-κB activity and chemokine production from a number of cell types, including MCs (Freedman and Shenoy, 2018; Walker et al., 2003). However, the possibility that βarr2 contributes to LL-37–induced

rosacea-like inflammation by modulating the phosphorylation status of cofilin and ERK1/2 and NF-κB activation has not been determined.

In this study, we investigated the status of MRGPRX2-expressing MCs in human patients with rosacea and determined the role of MrgprB2 in the development of experimental rosacea in mice. We further investigated the modulation of rosacea by βarr2 in vivo and its mechanism in vitro. The data presented in this study show that MrgprB2 expressed in MCs contributes to rosacea-like inflammation in mice and that βarr2 modulates this response by promoting MC chemotaxis through dephosphorylation of cofilin and cytokine/chemokine generation likely through ERK1/2 and NF-κB activation.

RESULTS

MRGPRX2-expressing MCs are present in normal skin, and their numbers are increased in patients with rosacea

To confirm previous reports that MC numbers are increased in the skin lesions of patients with rosacea (Aroni et al., 2008; Muto et al., 2014), we performed immunohistochemical analysis on skin biopsy samples using antitryptase antibody. We found that MC numbers are elevated in skin biopsy samples obtained from patients with rosacea compared with those in normal skin (Figure 1a and b). Because LL-37 activates human MCs through MRGPRX2 (Mascarenhas et al., 2017; Subramanian et al., 2011), we therefore sought to determine the status of MRGPRX2 in rosacea skin. Immunofluorescence staining of skin biopsy samples for MCs (antitryptase antibody, green) and MRGPRX2 (anti-MRGPRX2 antibody, red) showed that although MRGPRX2 is expressed in normal skin MCs, the number of MRGPRX2-expressing MCs (overlay image, yellow) are increased in rosacea skin (Figure 1c).

MrgprB2 contributes to LL-37–induced rosacea-like inflammation in mice

MrgprB2 is highly expressed in cutaneous MCs and has been identified as the mouse ortholog of human *MRGPRX2* (McNeil et al., 2015). Although LL-37 induces degranulation in human MCs through MRGPRX2 (Mascarenhas et al., 2017; Subramanian et al., 2011), the possibility that it activates murine MCs through MrgprB2 has not been tested. We therefore utilized mouse peritoneal MCs (PMCs) from wild-type (WT) and *MrgprB2*$^{-/-}$ mice and tested the effects of LL-37 and compound 48/80, a well-known MRGPRX2/B2 agonist, on calcium ion (Ca^{2+}) mobilization and degranulation. As shown in Figure 2a and c, compound 48/80–induced Ca^{2+} mobilization and degranulation were abolished in $^{MrgprB2^{-/-}}$ PMCs. Surprisingly, however, these responses to LL-37 were inhibited by ~50% (Figure 2b and c). To determine the roles of MrgprB2 and MCs on rosacea-like inflammation, we performed subcutaneous injection of LL-37 in WT, *MrgprB2*$^{-/-}$, and MC-deficient W^{sh}/W^{sh} mice and quantitated erythema at the injection site. LL-37–induced erythema was markedly inhibited (~70%) in *MrgprB2*$^{-/-}$ mice, and consistent with a previous report (Muto et al., 2014), this response was abolished in W^{sh}/W^{sh} mice compared with that in WT-mice (Figure 2d and e). These findings suggest that MRGPRB2 expressed in MCs substantially contributes to rosacea-like inflammation in mice.

LL-37–induced MC accumulation, expression of proinflammatory mediators, and immune cell recruitment require MrgprB2

The appearance of erythema in patients with rosacea and in rosacea-like inflammation in mice is associated with increased numbers of activated MCs (Kim et al., 2017; Muto et al., 2014; Yang et al., 2021). To determine the role of MrgprB2 on MC recruitment, we performed immunofluorescence staining with FITC-conjugated avidin, which selectively binds to MC granules. We found that LL-37 caused an increase in MC number in WT mice, but this response was significantly reduced in *MrgprB2*$^{-/-}$ mice (Figure 3a and b). The absence of avidin staining in the skin of vehicle- or LL-37–treated W^{sh}/W^{sh} mice shows its specificity for MC granules (Figure 3a).

MC activation in rosacea and rosacea-like inflammation in mice is associated with the expression of MC proteases such as matrix metalloproteinase 9 (MMP9), which cleaves its substrate produced from keratinocytes to generate LL-37, thus contributing to sustained MC activation in rosacea (Muto et al., 2014). In addition, chemokine CXCL2 produced by activated MCs drive the recruitment of inflammatory cells such as neutrophils in rosacea (Muto et al., 2014; Occhiuto et al., 2019). We found that LL-37 induces *Mmp9* and *Cxcl2* in WT mice, but these expressions were substantially reduced in *MrgprB2*$^{-/-}$ mice and absent in W^{sh}/W^{sh} mice (Figure 3c and d). Histological analysis of LL-37–injected H&E-stained skin sections showed reduced infiltration of inflammatory cells in *MrgprB2*$^{-/-}$ mice, and this response was absent in W^{sh}/W^{sh} mice (Figure 3e and Supplementary Figure S1).

βarr2 expressed in MCs contributes to the development of LL-37–induced rosacea

We previously showed that the absence of βarr2 in mouse PMCs results in enhanced degranulation in response to ciprofloxacin and antigen/IgE (Roy et al., 2019), but the role of this adapter protein in LL-37–induced responses is not known. We therefore utilized PMCs from WT and global βarr2-knockout (*βarr2*$^{-/-}$) mice and tested the ability of LL-37 to induce Ca^{2+} mobilization and degranulation. As shown in Figure 4a and b, both of these responses were enhanced in the absence of βarr2. Given that MCs are critical for the development of experimental rosacea, we used mice with MC-specific deletion of βarr2 (*Cpa3-Cre*$^{+}$*βarr2*$^{fl/fl}$) and respective control (*Cpa3-Cre*$^{-}$*βarr2*$^{fl/fl}$) mice to determine its in vivo implications. MC-specific deletion of βarr2 resulted in a significant decrease in LL-37–induced rosacea-like inflammation compared with that in control mice (Figure 4c and d). This reduction in erythema was associated with reduced MC accumulation (Figure 4e and f), *Mmp9* and *Cxcl2* expression (Figure 4g and h), and the recruitment of inflammatory cells (Figure 4i and Supplementary Figure S2).

βarr2 regulates LL-37–induced MC chemotaxis, cofilin dephosphorylation, and actin redistribution

LL-37 induces the chemotaxis of rodent and human MCs, indicating that increased MC number in rosacea likely reflects their recruitment rather than proliferation (Niyonsaba et al., 2002; Subramanian et al., 2011). To determine the role of βarr2 on MC chemotaxis in vitro, we utilized PMCs cultured from WT and *βarr2*$^{-/-}$ mice. Stimulation of WT PMCs with LL-37 resulted in a dose-dependent increase in chemotaxis, but this response was substantially reduced in *βarr2*$^{-/-}$ PMCs (Figure 5a). To determine whether βarr2 contributes

to MC chemotaxis by promoting cofilin dephosphorylation, we stimulated PMCs with LL-37 for different time points (0–30 minutes) and performed western blotting with an antibody that specifically recognizes cofilin phosphorylation at Ser-3. We found that in unstimulated WT PMCs, cofilin is present in its Ser-3–phosphorylated form and that after LL-37 stimulation, it undergoes rapid dephosphorylation (Figure 5b and c). However, this was reversed in *βarr2*$^{-/-}$ PMCs (Figure 5b and c). In addition, we used fluorescence microscopy in single cells (Figure 5d) and flow cytometry (Supplementary Figure S3) to confirm the western blotting data. To test whether LL-37–induced MC activation through MRGPRX2 promotes direct interaction of βarr2 with actin, we transiently transfected cDNA encoding βarr2 GFP (green) in rat basophilic leukemia 2H3 cells stably expressing MRGPRX2 and stained actin filament using Alexa Flour 546 phalloidin (red). As shown in Figure 5e, LL-37 stimulation caused rapid translocation of βarr2 to the cell periphery where it colocalizes with actin filament (yellow color). However, there was no colocalization in unstimulated cells as indicated by the absence of yellow color. These findings suggest that βarr2 contributes to LL-37–induced MC chemotaxis by its direct interaction with actin to promote cofilin dephosphorylation.

βarr2 modulates LL-37–induced ERK1/2 phosphorylation, NF-κB activation, and proinflammatory cytokine/chemokine generation

A previous study showed that LL-37 promotes ERK1/2 phosphorylation–dependent proinflammatory cytokine production (Niyonsaba et al., 2005). ERK1/2 is an upstream signaling protein of the transcription factor NF-κB, which is the master regulator of inflammatory processes in most immune cells, including MCs (Bilotta et al., 2021; Kim et al., 2005). NF-κB activation induces proinflammatory cytokines (such as TNF-α, IL-6, etc.) and chemokine (CCL3) from activated MCs, which induce neutrophil recruitment and inflammation (Kempuraj et al., 2003; Krystel-Whittemore et al., 2015). Because we found that βarr2 expressed in MCs modulates chemokine generation and rosacea-like inflammation in vivo (Figure 4), we sought to determine whether it also modulates LL-37–induced ERK1/2 phosphorylation, NF-κB activation, and cytokine/chemokine generation in vitro. We found that LL-37 stimulation resulted in time-dependent ERK1/2 phosphorylation in WT PMCs, but this response was significantly reduced in *βarr2*$^{-/-}$ cells (Figure 6a and b). NF-κB activation was assessed by determining the phosphorylation status of its p65 subunit. LL-37 caused enhanced phosphorylation of p65 in WT PMCs, but this response was significantly reduced in *βarr2*$^{-/-}$ cells (Figure 6a and b). This was further confirmed by immunofluorescence staining. LL-37 stimulation caused enhanced phosphorylated p65 staining (red color) in WT PMCs compared with that in *βarr2*$^{-/-}$ cells (Figure 6c). We also found that the absence of βarr2 resulted in a significant reduction in LL-37–induced generation of TNF-α, CCL3, and IL-6 (Figure 6d-f). These findings suggest that βarr2 participates in LL-37–induced ERK1/2 phosphorylation and NF-κB activation in MCs to promote rosacea-like inflammation in vivo through the generation of chemokine/cytokines (Figure 6).

DISCUSSION

It is generally accepted that the development of rosacea inflammation involves excessive generation of LL-37 and recruitment of leukocytes (Yamasaki and Gallo, 2009). Studies with human subjects and animal models strongly implicated MCs in the pathogenesis of rosacea (Aroni et al., 2008; Muto et al., 2014). However, identification of the MC receptor for LL-37 and its regulation remain poorly understood. The data presented in this study show that MRGPRX2-positive MCs are increased in the skin of patients with rosacea and that its murine counterpart, MrgprB2, substantially contributes to LL-37–induced rosacea-like inflammation in mice. We further showed that βarr2 expressed in MCs modulates this response by promoting LL-37–induced MC chemotaxis through the dephosphorylation of cofilin and inflammation likely through ERK1/2 and NF-κB activation.

McNeil et al. (2015) provided the first demonstration that of the 22 known Mas-related gene in mice, peritoneal and skin MCs express *Mrgprb2*. The original and subsequent findings that all cationic peptides that activate human MCs through MRGPRX2 also activate murine MCs through MrgprB2 led to the idea that it is the mouse ortholog of human MRGPRX2. However, the receptor through which LL-37 activates murine MCs has not been determined. We found that LL-37 induces robust Ca^{2+} mobilization and degranulation in WT PMCs, but these were reduced by ~50% in PMCs derived from *MrgprB2*$^{-/-}$ mice. Consistent with this, we found that whereas LL-37–induced *Mmp9/Cxcl2* expression, erythema, and rosacea-like inflammation were reduced in *MrgprB2*$^{-/-}$ mice, these responses were abolished in W^{sh}/W^{sh} mice. This suggests that MrgprB2 expressed in MCs does not fully account for the development of rosacea-like inflammation in mice. Recent RNA-sequencing data revealed the presence of other Mrgpr family member genes such as *Mrgprb1, Mrgprb8*, and *Mrgprb13* in murine skin MCs and PMCs (Dwyer et al., 2016; McNeil et al., 2015; Plum et al., 2020). Thus, the possibility that in addition to MrgprB2, one or more of these receptors contribute to rosacea-like inflammation in mice remains to be determined.

Our group previously showed that unlike other GPCRs expressed in MCs, MRGPRX2 is resistant to agonist-induced phosphorylation and desensitization (Subramanian et al., 2011). Subsequently, Chen et al. (2021) also showed that LL-37 does not cause βarr recruitment or MRGPRX2 desensitization. Despite this, we found that the absence of βarr2 enhances LL-37–induced Ca^{2+} mobilization and degranulation in mouse PMCs but inhibits cofilin dephosphorylation, ERK1/2 phosphorylation, NF-κB activation, and chemokine/chemokine generation. We previously showed that the absence of βarr2 enhances antigen/IgE-mediated MC degranulation, which does not require a GPCR activation (Roy et al., 2019). These findings suggest that the effects of βarr2 on LL-37–induced responses in MCs are mediated independently of receptor phosphorylation and desensitization. Although the data presented in this study suggest that βarr2 contributes to the development of LL-37-induced rosacea-like inflammation by promoting MC chemotaxis and generation of chemokines, the significance of its ability to attenuate early MC degranulation is not clear. It is noteworthy that LL-37 and other antimicrobial peptides generated from host cells in response to microbial infection promote host defense by at least two mechanisms: one involving the direct killing of microbes and the other by harnessing MC's immunomodulatory properties (Amponnawarat et al., 2021; Arifuzzaman et al., 2019). Thus, it is tempting to speculate

that βarr2 plays a dual role in LL-37–induced MC response; it attenuates host defense but promotes rosacea-like inflammation.

For certain GPCRs, βarr2 orchestrates cytoskeletal rearrangement and cell migration by modulating the phosphorylation and dephosphorylation status of the actin depolymerization factor cofilin (McGovern and DeFea, 2014; Zoudilova et al., 2010). Cofilin phosphorylation at Ser-3 causes its inactivation, whereas dephosphorylation promotes its activation (Zoudilova et al., 2010, 2007). The finding of this study that βarr2 colocalizes with F-actin and that the absence of βarr2 results in substantial inhibition of LL-37–induced chemotaxis and that this is associated with enhanced cofilin phosphorylation supports the notion that βarr2-mediated cofilin dephosphorylation promotes MC chemotaxis. In a variety of cell types, βarr2 forms a signaling complex with the phosphatase (chronophin) and LIM kinase to regulate the phosphorylation/dephosphorylation status of cofilin (DeFea, 2013). Whether these protein kinases or phosphatases form a signaling complex with βarr2 to modulate MC recruitment in rosacea remains to be determined.

βarr2 contributes to ERK1/2 phosphorylation in response to the stimulation of β-adrenergic receptor (Niyonsaba et al., 2005; Shenoy et al., 2006). Moreover, βarr2 positively or negatively modulates NF-κB–mediated cellular responses depending on the cell type and the receptor involved (Freedman and Shenoy, 2018; Gaffal et al., 2014; Sun and Lin, 2008). NF-κB was shown to be upregulated in rosacea-like skin inflammation and could be used as a therapeutic target to mitigate rosacea (Chen et al., 2019; Deng et al., 2021). In this study, we showed that MC-specific deletion of βarr2 resulted in a significant reduction of *Cxcl2* expression and rosacea-like inflammation in vivo. Furthermore, LL-37–induced ERK1/2, p65 phosphorylation, and proinflammatory cytokine/chemokine generation were significantly reduced in the absence of βarr2 in MCs in vitro. These findings in total suggest that βarr2 expressed in MCs contributes to the development of rosacea by modulating both MC chemotaxis and the generation of proinflammatory cytokines.

In conclusion, this study showed a potential role of MRGPRX2 and MrgprB2 in the development of human rosacea as well as in LL-37–induced rosacea-like skin inflammation in mice. Furthermore, βarr2 expressed in MCs contributes to rosacea by modulating MC chemotaxis and chemokine/cytokine gene expression. Thus, MRGPRX2 and βarr2 could be targeted for therapeutic intervention for the treatment of rosacea.

MATERIALS AND METHODS

Healthy and rosacea skin samples

Normal and rosacea skin samples were obtained from the Skin Biology and Diseases Resource-Based Center at the University of Pennsylvania (Philadelphia, PA). The protocol for tissue procurement was approved by the University of Pennsylvania Institutional Review Board, and all donors provided written informed consent.

Mice

C57BL/6 (WT), MC-deficient (W^{sh}/W^{sh}), and global βarr2-knockout ($\beta arr2^{-/-}$) mice were obtained from The Jackson Laboratory (Bar Harbor, ME). βarr2 flox/flox ($\beta arr2^{fl/fl}$) mice

were a kind gift from Robert Lefkowitz and Julia Walker (Duke University Medical Center, Durham, NC); *Cpa3-Cre* (Cre is expressed under the promoter of Cpa3, expressed only in MCs) mice were generously provided by Stephen J. Galli (Stanford University, Stanford, CA). Mice were housed in pathogen-free cages on autoclaved hardwood bedding. Mice with MC-specific deletion of βarr2 (*Cpa3-Cre*$^{+}$/*βarr2*$^{fl/fl}$) were generated as described earlier by crossing *Cpa3-Cre* mice with *βarr2*$^{fl/fl}$ mice (Roy et al., 2019). *MrgprB2*$^{-/-}$ mice were generated through CRISPR/Cas9 by the CRISPR Core of the University of Pennsylvania (Alkanfari et al., 2019). Mice aged 8–12 weeks were used in the entire study. All experiments were approved by the Institutional Animal Care and Use Committee at the University of Pennsylvania.

Quantitative real-time PCR

Skin samples were homogenized, and total RNA was extracted and purified by RNeasy Fibrous Tissue Kit (Qiagen, Hilden, Germany). A total of 1 mg of RNA was used to synthesize cDNA using the High-Capacity RNA-to-cDNA Kit (Applied Biosystem, Foster City, CA) according to the manufacturer's instructions. Using TaqMan Gene Expression Assays primers, the mRNA expressions of mouse *Mmp9* and *Cxcl2* were analyzed using QuantStudio 3 Real-Time PCR System (Thermo Fisher Scientific, Waltham, MA). The analysis was performed in triplicate, and *Gapdh* was used as an internal control. All data are presented as fold changes to control (Roy et al., 2019).

ELISA

Cytokine production was measured as described previously (Amponnawarat et al., 2021). Briefly, PMCs (0.5×10^6/ml) from WT and *βarr2*$^{-/-}$ mice were incubated with LL-37 (10 μM) in complete Iscove's Modified Dulbecco's Medium for 16 hours. Cells were centrifuged, and supernatants were collected and stored frozen at −80 °C until analysis. IL-6, TNF-α, and CCL3 cytokine/chemokine levels were quantified by a sandwich ELISA kit (R&D Systems, Minneapolis, MN) according to the manufacturer's instructions.

Western blotting

Western blotting in WT and *βarr2*$^{-/-}$ PMCs was performed similarly as described earlier (Roy et al., 2019). PMCs were stimulated with LL-37 (10 μM) at different time points (0–30 minutes), and cell lysate was prepared. Protein was separated in SDS-PAGE, transferred to polyvinylidene difluoride membrane, and incubated overnight with respective antibodies (1:1,000) in blocking buffer (5% skim milk in 0.1% Tris-buffered saline with 0.1% Tween 20 detergent). This was followed by incubation with horseradish peroxidase–conjugated anti-rabbit or anti-mouse IgG (1:1,000) and was developed using Pico plus Chemiluminescence Substrate. Blots were restriped and probed with respective total antibodies. Image was acquired in iBright 1500 Imaging System (Thermo Fisher Scientific) and analyzed in ImageJ software, version 1.52a (National Institutes of Health, Bethesda, MD).

In vivo

WT (C57BL/6), MC-deficient (W^{sh}/W^{sh}), *MrgprB2*$^{-/-}$, *Cpa3-Cre*$^{-}$/*βarr2*$^{fl/fl}$, and *Cpa3-Cre*$^{+}$/*βarr2*$^{fl/fl}$ mice were used for in vivo rosacea model as stated earlier (Yuan et al., 2019). Mice were shaved 24 hours before the experiment. Experimental and control groups were intradermally injected with either LL-37 (320 μM, 50 μl) or PBS, respectively, twice a day for 2 consecutive days. Dorsal skin was evaluated for the degree of inflammation and then excised after 72 hours of the first injection. The excised tissue was either immersed immediately into 10% formalin for histology or in RNAlater Solution (Invitrogen, Carlsbad, CA) and stored for qPCR.

Statistical analysis

Data shown are mean ± SEM values derived from at least three independent experiments. Statistical significance was determined by one-way or two-way ANOVA and nonparametric *t*-test. Error bars represent mean ± SEM from three independent experiments. Significant differences were set at $*P \leq 0.05$, $**P \leq 0.01$, and $***P \leq 0.001$ and analyzed by GraphPad Prism, version 6.07.

Supplementary Material

Refer to Web version on PubMed Central for supplementary material.

ACKNOWLEDGMENT

We are thankful to the Skin Biology and Diseases Resource-Based Center at the University of Pennsylvania for providing patients with rosacea and respective control skin samples. We thank the Tissue Processing core facility of the School of Dental Medicine, University of Pennsylvania for histological sample preparation, sectioning, and staining. We also thank the confocal microscopy core facility at the School of Dental Medicine, University of Pennsylvania for image acquisition. This work was supported by National Institutes of Health grants R01-AI124182, R01-AI143185, and R01-AI149487 to HA.

Data availability statement

All datasets generated for this study are included in the article/ Supplementary Materials and Methods.

Abbreviations:

βarr	β-arrestin
Ca^{2+}	calcium ion
ERK1/2	extracellular signal–regulated kinase 1/2
GPCR	G protein—coupled receptor
MC	mast cell
MMP9	matrix metalloproteinase 9
PMC	peritoneal mast cell

WT wild-type

REFERENCES

Alkanfari I, Freeman KB, Roy S, Jahan T, Scott RW, Ali H. Small-molecule host-defense peptide mimetic antibacterial and antifungal agents activate human and mouse mast cells via Mas-related GPCRs. Cells 2019;8:311.

Amponnawarat A, Chompunud NA, Ayudhya C, Ali H. Murepavadin, a small molecule host defense peptide mimetic, activates Mast cells via MRGPRX2 and MrgprB2. Front Immunol 2021;12:689410. [PubMed: 34248979]

Arifuzzaman M, Mobley YR, Choi HW, Bist P, Salinas CA, Brown ZD, et al. MRGPR-mediated activation of local mast cells clears cutaneous bacterial infection and protects against reinfection. Sci Adv 2019;5:eaav0216. [PubMed: 30613778]

Aroni K, Tsagroni E, Kavantzas N, Patsouris E, Ioannidis E. A study of the pathogenesis of rosacea: how angiogenesis and mast cells may participate in a complex multifactorial process. Arch Dermatol Res 2008;300:125–31. [PubMed: 18071725]

Bilotta S, Paruchuru LB, Feilhauer K, Köninger J, Lorentz A. Resveratrol is a natural inhibitor of human intestinal mast cell activation and phosphorylation of mitochondrial ERK1/2 and STAT3. Int J Mol Sci 2021;22:7640. [PubMed: 34299258]

Callahan BN, Kammala AK, Syed M, Yang C, Occhiuto CJ, Nellutla R, et al. Osthole, a natural plant derivative inhibits MRGPRX2 induced mast cell responses. Front Immunol 2020;11:703. [PubMed: 32391014]

Chen E, Chuang LS, Giri M, Villaverde N, Hsu NY, Sabic K, et al. Inflamed ulcerative colitis regions associated with MRGPRX2-mediated mast cell degranulation and cell activation modules, defining a new therapeutic target. Gastroenterology 2021;160:1709–24. [PubMed: 33421512]

Chen M, Xie H, Chen Z, Xu S, Wang B, Peng Q, et al. Thalidomide ameliorates rosacea-like skin inflammation and suppresses NF-κB activation in keratinocytes. Biomed Pharmacother 2019;116:109011. [PubMed: 31132668]

Choi JE, Werbel T, Wang Z, Wu CC, Yaksh TL, Di Nardo A. Botulinum toxin blocks mast cells and prevents rosacea like inflammation. J Dermatol Sci 2019;93:58–64. [PubMed: 30658871]

DeFea KA. Arrestins in actin reorganization and cell migration. Prog Mol Biol Transl Sci 2013;118:205–22. [PubMed: 23764055]

Deng Z, Chen M, Liu Y, Xu S, Ouyang Y, Shi W, et al. A positive feedback loop between mTORC1 and cathelicidin promotes skin inflammation in rosacea. EMBO Mol Med 2021;13:e13560. [PubMed: 33734592]

Dondalska A, Rönnberg E, Ma H, Pålsson SA, Magnusdottir E, Gao T, et al. Amelioration of compound 48/80-mediated itch and LL-37-Induced inflammation by a single-stranded oligonucleotide. Front Immunol 2020;11:559589. [PubMed: 33101278]

Dwyer DF, Barrett NA, Austen KF, Immunological Genome Project Consortium. Expression profiling of constitutive mast cells reveals a unique identity within the immune system. Nat Immunol 2016;17:878–87. [PubMed: 27135604]

Freedman NJ, Shenoy SK. Regulation of inflammation by β-arrestins: not just receptor tales. Cell Signal 2018;41:41–5. [PubMed: 28189586]

Gaffal E, Jakobs M, Glodde N, Schröder R, Kostenis E, Tüting T. β-arrestin 2 inhibits proinflammatory chemokine production and attenuates contact allergic inflammation in the skin. J Invest Dermatol 2014;134:2131–7. [PubMed: 24577407]

Kanada KN, Nakatsuji T, Gallo RL. Doxycycline indirectly inhibits proteolytic activation of tryptic kallikrein-related peptidases and activation of cathelicidin. J Invest Dermatol 2012;132:1435–42. [PubMed: 22336948]

Kempuraj D, Huang M, Kandere-Grzybowska K, Basu S, Boucher W, Letourneau R, et al. Azelastine inhibits secretion of IL-6, TNF-alpha and IL-8 as well as NF-kappaB activation and intracellular calcium ion levels in normal human mast cells. Int Arch Allergy Immunol 2003;132:231–9. [PubMed: 14646384]

Kim M, Kim J, Jeong SW, Jo H, Woo YR, Park HJ. Inhibition of mast cell infiltration in an LL-37-induced rosacea mouse model using topical brimonidine tartrate 0.33% gel. Exp Dermatol 2017;26:1143–5. [PubMed: 28500634]

Kim MS, Lim WK, Park RK, Shin T, Yoo YH, Hong SH, et al. Involvement of mitogen-activated protein kinase and NF-kappaB activation in Ca2+-induced IL-8 production in human mast cells. Cytokine 2005;32:226–33. [PubMed: 16343928]

Krystel-Whittemore M, Dileepan KN, Wood JG. Mast cell: a multi-functional master cell. Front Immunol 2015;6:620. [PubMed: 26779180]

Mascarenhas NL, Wang Z, Chang YL, Di Nardo A. TRPV4 mediates mast cell activation in cathelicidin-induced rosacea inflammation. J Invest Dermatol 2017;137:972–5. [PubMed: 27908695]

McGovern KW, DeFea KA. Molecular mechanisms underlying beta-arrestin-dependent chemotaxis and actin-cytoskeletal reorganization. Handb Exp Pharmacol 2014;219:341–59. [PubMed: 24292838]

McNeil BD, Pundir P, Meeker S, Han L, Undem BJ, Kulka M, et al. Identification of a mast-cell-specific receptor crucial for pseudo-allergic drug reactions. Nature 2015;519:237–41. [PubMed: 25517090]

Muto Y, Wang Z, Vanderberghe M, Two A, Gallo RL, Di Nardo A. Mast cells are key mediators of cathelicidin-initiated skin inflammation in rosacea. J Invest Dermatol 2014;134:2728–36. [PubMed: 24844861]

Niyonsaba F, Iwabuchi K, Someya A, Hirata M, Matsuda H, Ogawa H, et al. A cathelicidin family of human antibacterial peptide LL-37 induces mast cell chemotaxis. Immunology 2002;106:20–6. [PubMed: 11972628]

Niyonsaba F, Ushio H, Hara M, Yokoi H, Tominaga M, Takamori K, et al. Antimicrobial peptides human beta-defensins and cathelicidin LL-37 induce the secretion of a pruritogenic cytokine IL-31 by human mast cells. J Immunol 2010;184:3526–34. [PubMed: 20190140]

Niyonsaba F, Ushio H, Nagaoka I, Okumura K, Ogawa H. The human beta-defensins (−1, −2, −3, −4) and cathelicidin LL-37 induce IL-18 secretion through p38 and ERK MAPK activation in primary human keratinocytes. J Immunol 2005;175:1776–84. [PubMed: 16034119]

Occhiuto CJ, Kammala AK, Yang C, Nellutla R, Garcia M, Gomez G, et al. Store-operated calcium entry via STIM1 contributes to MRGPRX2 induced mast cell functions. Front Immunol 2019;10:3143. [PubMed: 32038646]

Plum T, Wang X, Rettel M, Krijgsveld J, Feyerabend TB, Rodewald HR. Human mast cell proteome reveals unique lineage, putative functions, and structural basis for cell ablation. Immunity 2020;52:404–16.e5. [PubMed: 32049054]

Roy S, Chompunud Na Ayudhya CC, Thapaliya M, Deepak V, Ali H. Multifaceted MRGPRX2: new insight into the role of mast cells in health and disease. J Allergy Clin Immunol 2021;148:293–308. [PubMed: 33957166]

Roy S, Gupta K, Ganguly A, Ali H. β-Arrestin2 expressed in mast cells regulates ciprofloxacin-induced pseudoallergy and IgE-mediated anaphylaxis. J Allergy Clin Immunol 2019;144:603–6. [PubMed: 31077686]

Shenoy SK, Drake MT, Nelson CD, Houtz DA, Xiao K, Madabushi S, et al. beta-arrestin-dependent, G protein-independent ERK1/2 activation by the beta2 adrenergic receptor. J Biol Chem 2006;281:1261–73. [PubMed: 16280323]

Subramanian H, Gupta K, Guo Q, Price R, Ali H. Mas-related gene X2 (MrgX2) is a novel G protein-coupled receptor for the antimicrobial peptide LL-37 in human mast cells: resistance to receptor phosphorylation, desensitization, and internalization. J Biol Chem 2011;286:44739–49. [PubMed: 22069323]

Sun J, Lin X. Beta-arrestin 2 is required for lysophosphatidic acid-induced NF-kappaB activation. Proc Natl Acad Sci USA 2008;105:17085–90. [PubMed: 18952848]

Walker JK, Fong AM, Lawson BL, Savov JD, Patel DD, Schwartz DA, et al. Beta-arrestin-2 regulates the development of allergic asthma. J Clin Invest 2003;112:566–74. [PubMed: 12925697]

Yamasaki K, Di Nardo A, Bardan A, Murakami M, Ohtake T, Coda A, et al. Increased serine protease activity and cathelicidin promotes skin inflammation in rosacea. Nat Med 2007;13:975–80. [PubMed: 17676051]

Yamasaki K, Gallo RL. The molecular pathology of rosacea. J Dermatol Sci 2009;55:77–81. [PubMed: 19481425]

Yang L, Shou YH, Yang YS, Xu JH. Elucidating the immune infiltration in acne and its comparison with rosacea by integrated bioinformatics analysis. PLoS One 2021;16:e0248650. [PubMed: 33760854]

Yuan X, Li J, Li Y, Deng Z, Zhou L, Long J, et al. Artemisinin, a potential option to inhibit inflammation and angiogenesis in rosacea. Biomed Pharmacother 2019;117:109181. [PubMed: 31387196]

Zoudilova M, Kumar P, Ge L, Wang P, Bokoch GM, DeFea KA. Beta-arrestin-dependent regulation of the cofilin pathway downstream of protease-activated receptor-2. J Biol Chem 2007;282:20634–46. [PubMed: 17500066]

Zoudilova M, Min J, Richards HL, Carter D, Huang T, DeFea KA. beta-arrestins scaffold cofilin with chronophin to direct localized actin filament severing and membrane protrusions downstream of protease-activated receptor-2. J Biol Chem 2010;285:14318–29. [PubMed: 20207744]

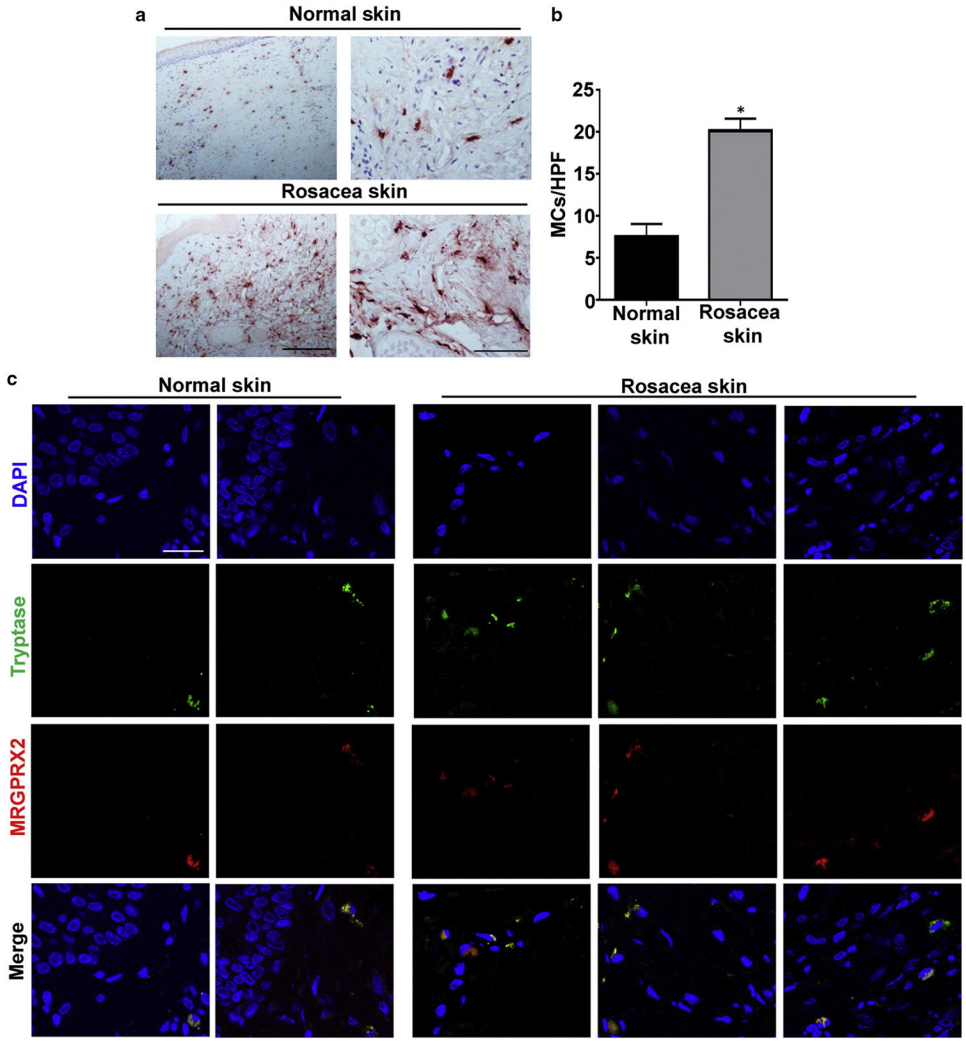

Figure 1. MRGPRX2-expressing MC numbers are increased in the skin of patients with rosacea.

(**a**) Immunohistochemistry was performed in skin samples (healthy individuals and patients with rosacea) by staining with antitryptase antibody, and representative tissue samples were shown. Bar = 50 μm (left) and 200 μm (right). (**b**) Quantitative analysis was done by counting the MC numbers in a total of 15 HPFs from five different tissue sections of both healthy and rosacea skin. (**c**) Representative immunofluorescence staining of MRGPRX2 and tryptase from two healthy and three rosacea skin samples was shown. Bar = 20 μm. MRGPRX2 is shown in red, tryptase is shown in green, and DAPI is shown in blue. HPF, high-power field; MC, mast cell.

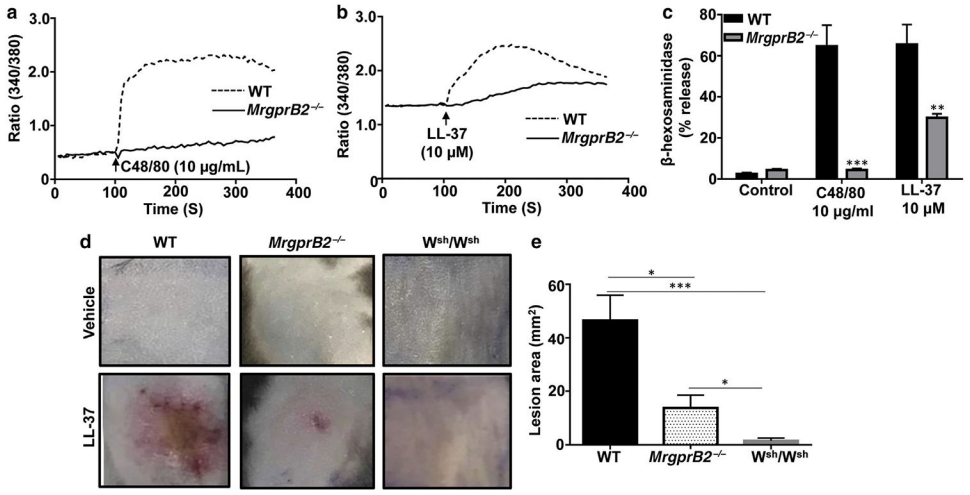

Figure 2. MrgprB2 contributes to LL-37–induced MC activation in vitro and rosacea-like skin inflammation in vivo.

(**a, b**) WT and *MrgprB2*$^{-/-}$ PMCs were loaded with Fura 2 AM, and the time course of Ca^{2+} mobilization was measured for 5 min after being stimulated with C48/80 and LL-37. (**c**) PMCs were stimulated with the indicated concentrations of C48/80 and LL-37, and β-hexosaminidase release was measured. (**d**) PBS (vehicle) or LL-37 (320 μM, 50 μl) was intradermally injected in WT, *MrgprB2*$^{-/-}$, and W^{sh}/W^{sh} mice (6–7 per group) twice daily for 2 consecutive days, and erythema was measured. A representative image of dorsal skin and (**e**) lesion size (mm^2) was measured. C48/80, compound 48/80; Ca^{2+}, calcium ion; MC, mast cell; min, minute; PMC, peritoneal mast cell; WT, wild-type.

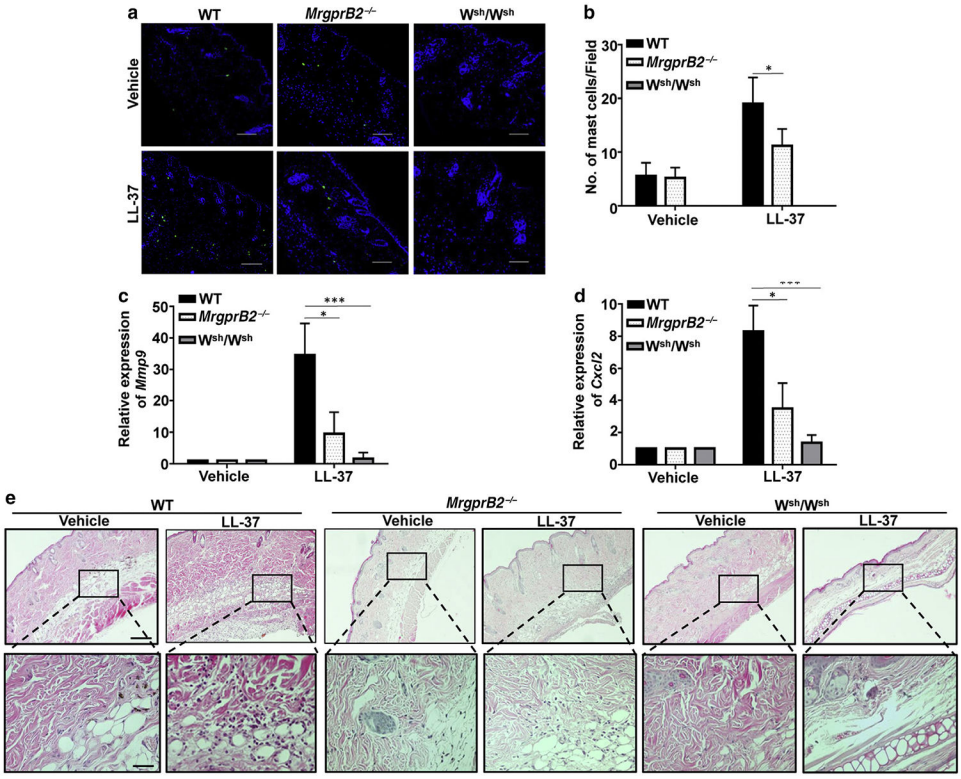

Figure 3. LL-37–mediated MC recruitment, induction of *Mmp9* and *Cxcl2* transcripts, and inflammation are reduced in *MrgprB2*$^{-/-}$ mice.

Skin tissue was excised from WT, *MrgprB2*$^{-/-}$, and W^{sh}/W^{sh} mice and processed. (**a**) A representative image showing avidin-stained (green) MCs and DAPI (blue)-stained nucleus in the skin tissue. Bar = 50 μm. (**b**) Quantitative analysis of MC number in the skin. mRNA transcripts level of (**c**) *Mmp9* and (**d**) *Cxcl2* was determined by qPCR. (**e**) Skin tissue was stained with H&E for immune cell infiltration. Bar = 100 μm (top panel) and 50 μm (bottom panel). MC, mast cell; MMP9, matrix metalloproteinase 9; WT, wild-type.

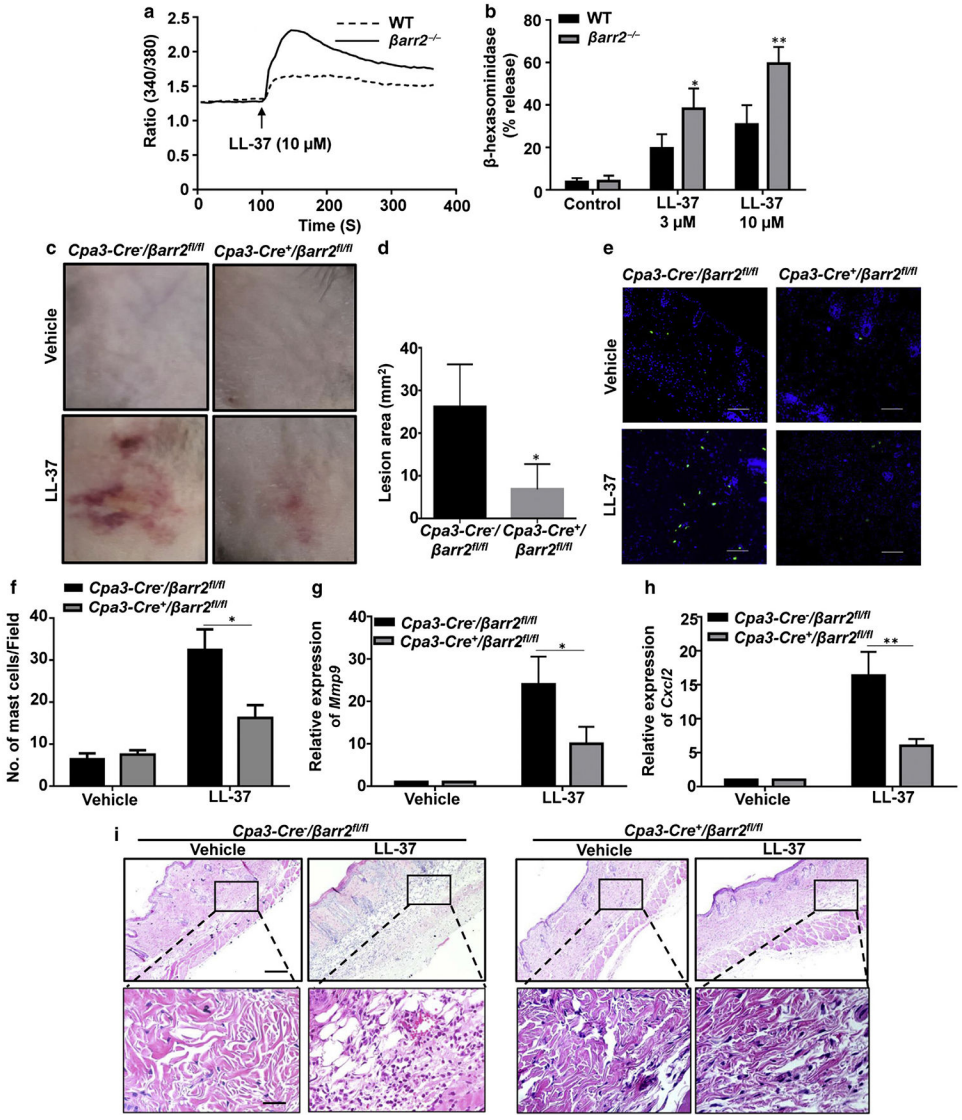

Figure 4. βarr2 differentially regulates early LL-37–induced MC activation in vitro and delayed rosacea-like inflammation in vivo.

(**a**) Fura-2–loaded WT and *βarr2*$^{-/-}$ PMCs were exposed to LL-37, and the time course of Ca^{2+} mobilization was measured for 5 mins. (**b**) Cells were stimulated with LL-37 for 30 mins, and degranulation (as measured by β-hexosaminidase release) was quantitated. (**c**) A representative image of LL-37–induced rosacea-like inflammation in control mice (*Cpa3-Cre*$^{-}$*/βarr2*$^{fl/fl}$) and mice with MC-specific deletion of βarr2 (*Cpa3-Cre*$^{+}$*/βarr2*$^{fl/fl}$). (**d**) Quantitation of lesion size (mm^2). (**e**) MC staining. Bar = 50 μm. (**f**) Quantitative MC number. qPCR analysis of (**g**) *Mmp9* and (**h**) *Cxcl2* and (**i**) H&E staining are shown. Bar = 100 μm (top panel) and 50 μm (bottom panel). μarr2, β-arrestin 2; Ca^{2+}, calcium ion; MC, mast cell; min, minute; MMP9, matrix metalloproteinase 9; PMC, peritoneal mast cell; WT, wild-type.

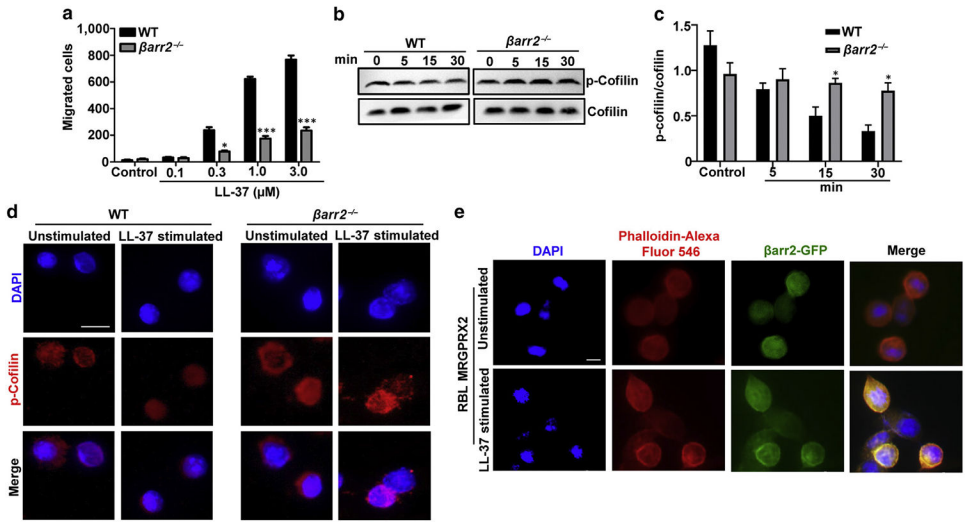

Figure 5. βarr2 regulates LL-37–induced MC chemotaxis, cofilin dephosphorylation, and actin reorganization.

(**a**) PMCs from WT and global *βarr2*$^{-/-}$ mice were stimulated with LL-37 (0–3 μM), and a chemotaxis assay was performed. (**b**) PMCs were stimulated with LL-37 (10 μM) for 0–30 mins, and western blotting was performed with antiphosphorylated cofilin (Ser-3) antibody to determine cofilin phosphorylation. Blot was stripped and reprobed with an anticofilin antibody to determine total protein. Representative western blots are shown. (**c**) Bar graphs showing the relative intensities of phosphoprotein normalized to total protein. (**d**) PMCs were stimulated with LL-37 (10 μM) for 10 mins, fixed, permeabilized, and stained with antiphosphorylated cofilin antibody followed by Alexa Fluor 594–conjugated secondary antibody. Cofilin phosphorylation was visualized in fluorescent microscopy. Bar = 50 μm. (**e**) βarr2 GFP–transfected RBL-MRGPRX2 cells were stimulated with LL-37 (1 μM) for 10 mins, and actin filament was stained with Alexa Fluor 546–conjugated phalloidin. Colocalization of βarr2 with actin was visualized in fluorescent microscopy. Bar = 50 μm. βarr2, β-arrestin 2; MC, mast cell; min, minute; PMC, peritoneal mast cell; RBL, rat basophilic leukemia; WT, wild-type.

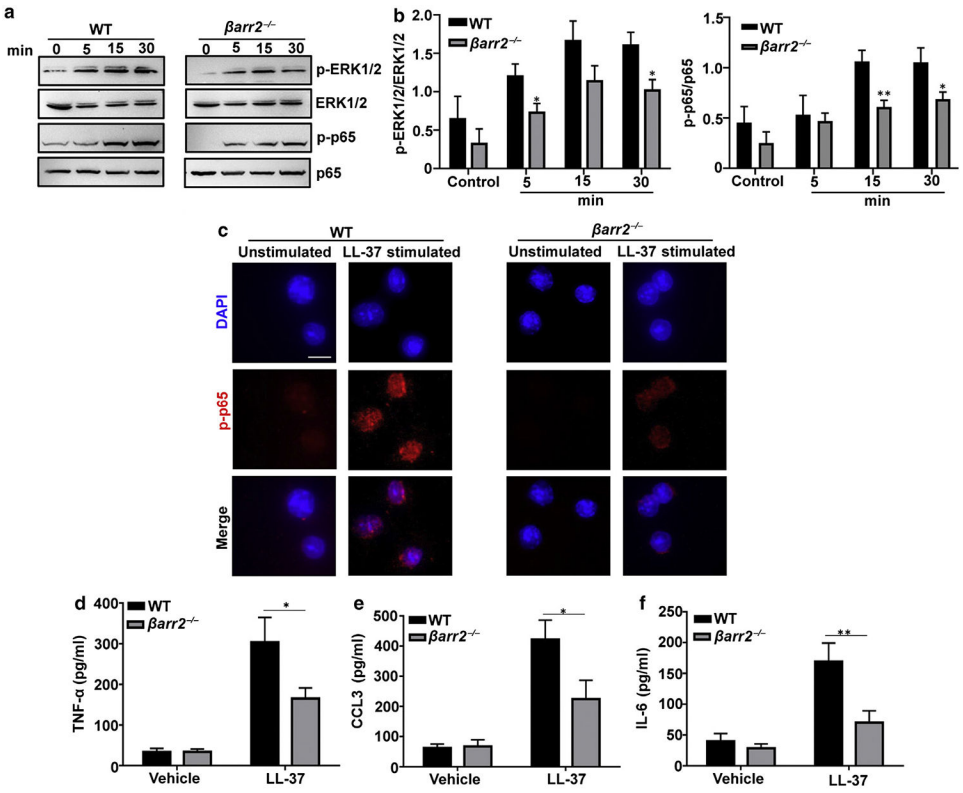

Figure 6. βarr2 regulates NF-κB activation and proinflammatory cytokines/chemokine production in mouse PMCs.

(**a**) WT and *βarr2*$^{-/-}$ PMCs were stimulated with LL-37 (10 μM) for 0–30 mins, and western blotting was performed for p-ERK1/2 (Thr202/Tyr204) and NF-κB p-p65 (Ser 536) subunits. Blots were stripped and reprobed with total anti-ERK1/2 and anti-p65 antibodies to determine total proteins and representative images are shown. (**b**) Bar graphs show the relative intensity of phosphoprotein normalized to total protein. (**c**) PMCs were stimulated with LL-37 (10 μM) for 10 mins, fixed, permeabilized, and stained with anti–p-p65 antibody, followed by staining with Alexa Fluor 594–conjugated secondary antibody. NF-κB p65 phosphorylation was visualized by fluorescent microscopy. Bar = 50 μm. PMCs (0.5×10^6) were stimulated with LL-37 (10 μM) for 16 h, and the supernatant was collected. ELISA for (**d**) TNF-α, (**e**) CCL3, and (**f**) IL-6 was performed. Cytokine/chemokine secretion is presented as pg/ml. βarr2, β-arrestin 2; ERK, extracellular signal–regulated kinase 1/2; h, hour; min, minute; p-ERK1/2, phosphorylated extracellular signal–regulated kinase 1/2; PMC, peritoneal mast cell; p-p65, phosphorylated p65; WT, wild-type.